Electronic Supplementary Material (ESI) for Inorganic Chemistry Frontiers.


# Electronic Supplementary Information

# Surface modification of Li-rich manganese-based cathode materials by chemical etching

Heng Cui, Hang Li, Jiuding Liu, Yudong Zhang, Fangyi Cheng* and Jun Chen

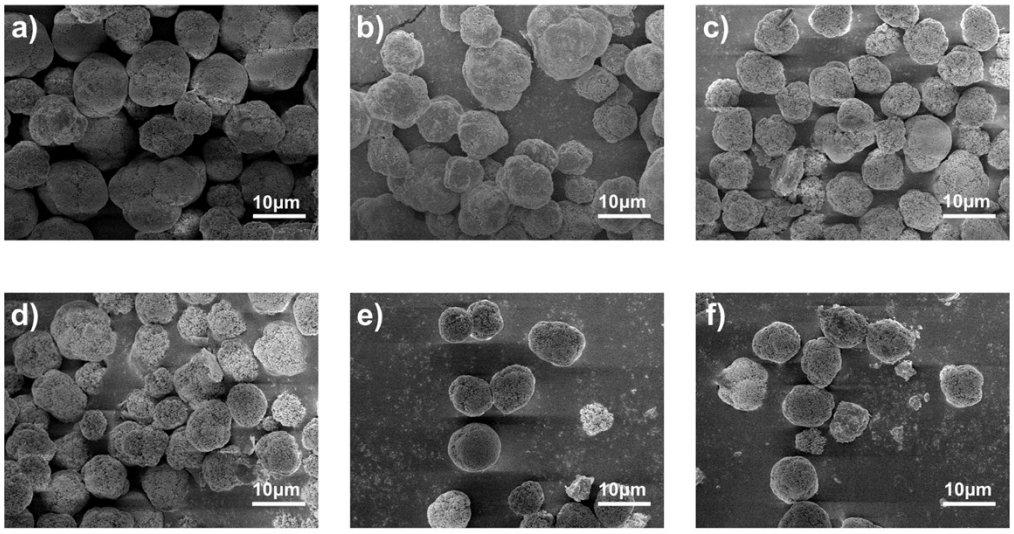


**Fig. S1** SEM images of precursors in different co−precipitation reaction times. (a) 11h, (b) 12h, (c) 13h, (d) 14h, (e) 15h and (f) 16h.

To select the best settling time, SEM was applied to observe the morphology of the precursors every 1 h after 11 h co−precipitation. As the results shown in **Figure S1**, 15 h is the time when the precursors become a uniform spheres.

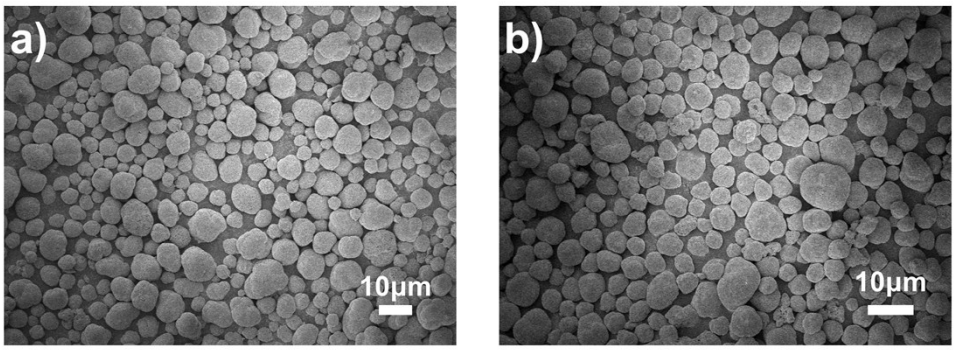


**Figure S2** The SEM images of LMCN (a) and CLMCN (b).

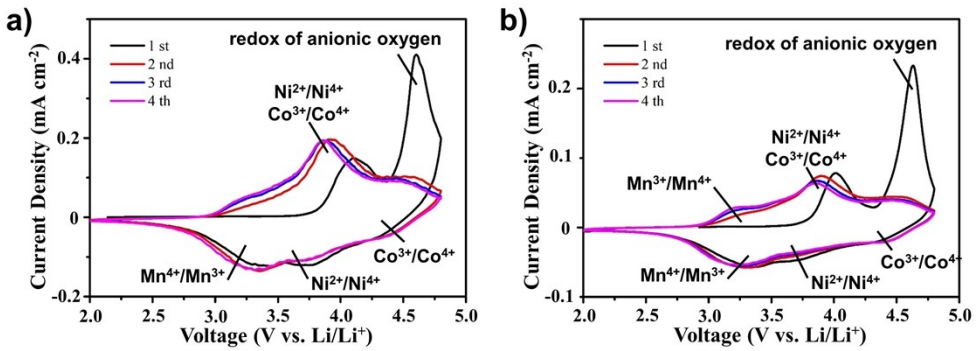


**Fig. S3** CV curves for the initial four cycles of LMCN (a) and CLMCN (b).

Cyclic voltammogram (CV) test was conducted between 2.0–4.8 V at a scanning rate of 0.1 mV $s^{-1}$ using a Ivium−n−State multichannel electrochemical analyser (IVIUM). As shown in **Figure S3**, peak at 4.11V in initial charging process of LMCN corresponds to the redox of transition metal, shifts to 4.00 V after etched, which results from the increase of $Mn^{3+}$ in the amorphous layer.[1,2] Besides, in the initial discharging process, the intensity of peak at 3.7 V, which represent the reduction of $Ni^{4+}$, reduces after chemical etching, indicating the decrease of Ni in the surface.[1,3] In the following charging process, CLMCN represents a more obvious peak at 3.2 V that implies the oxidation of Mn, which correspond to dQ/dV profiles.

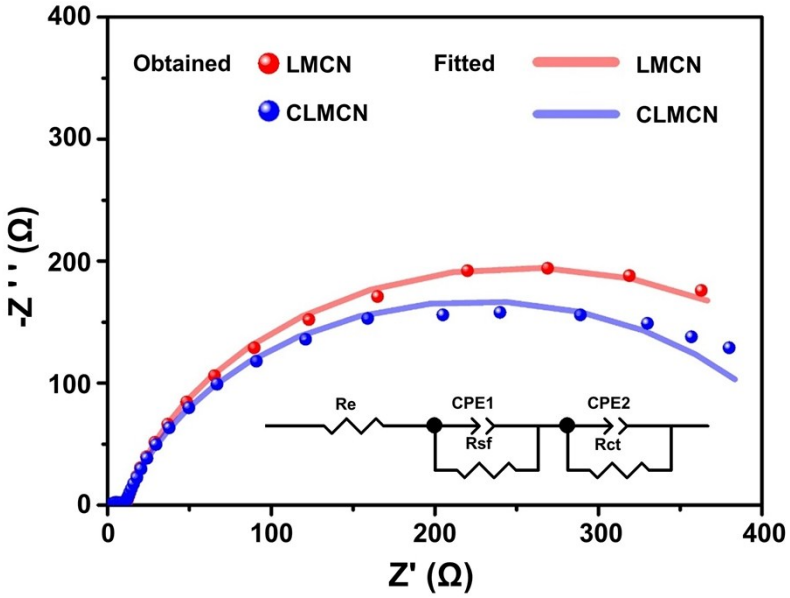


**Fig. S4** EIS spectra with charged for 4.8 V after 100 cycles. The equivalent circuit model for the electrochemical impedance fitting are placed under the curves.

Electrochemical impedance spectroscopy (EIS) was conducted using IVIUM at a

frequency ranged from 10 mHz to 100 kHz after 100 cycles charged. The EIS spectra of the LMCN and CLMCN are shown in **Figure S4**. Both Nyquist plots of the two samples are similar with two semicircles portion. The first semicircle occurred at high frequency is related to the resistance of surface film ($R_{sf}$) and the second semicircle at low frequency is attributed to the resistance of charge transfer ($R_{ct}$) at the interface between the electrolyte and electrode. Fitting the Nyquist plots with the equivalent circuit model as shown in **Figure S4**, the equivalent values of $R_{sf}$ and $R_{ct}$ are summarized in **Table S1**. $R_{sf}$ of CLMCN is slightly higher than that of LMCN after cycling, which is associated with the poor electrical conductivity of the amorphous layer. On the other hand, $R_{ct}$ of CLMCN is lower than that of LMCN, implying chemical etching can protect the active sites in the surface during cycling, which can be ascribed to the reduce of side reaction and enhance the structure in the surface.[4]

**Table S1** Impedance fitting parameters of surface film resistance ($R_{sf}$) and charge transfer resistance ($R_{ct}$) for LMCN and CLMCN.

| | LMCN | CLMCN |
|---|---|---|
| $R_{sf}$ ( Ω ) | 10.26 | 484.6 |
| $R_{ct}$ ( Ω ) | 19.54 | 387.8 |

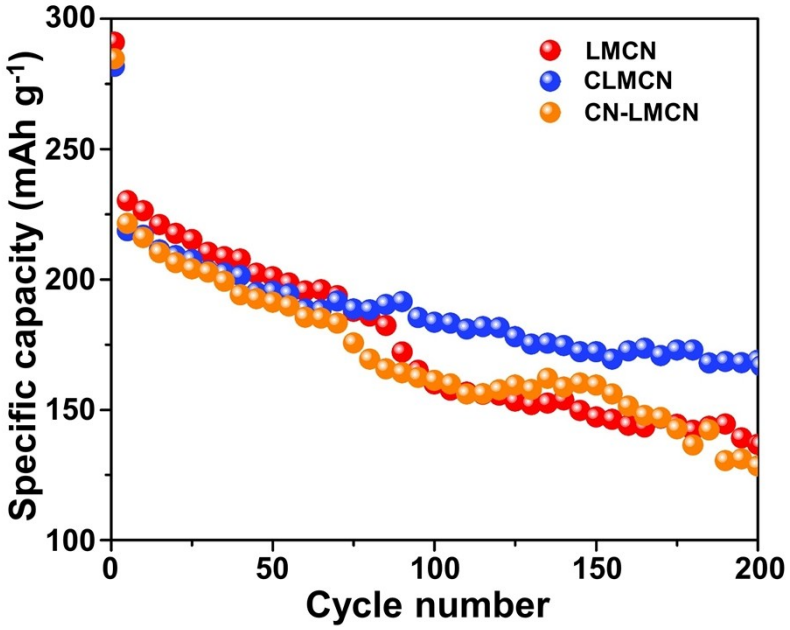


**Fig. S5** Cycling performance of pristine, CAN−etched and CN−treated LMCN samples. The electrodes were charged/discharged at 0.1 C in the initial two cycles and at 1 C in following cycles.

Clearly, CAN-etched sample exhibited better capacity retention than both LMCN and CN-treated samples. Considering that Ce-based species are also generated by treatment with $Ce(NO_3)_3$, the enhanced electrochemical performance of CAN-treated cathode material is mainly attributed to strong oxidizing ability of CAN, which modifies the composition and oxidation state of transition metal and oxygen species on the surface of LMCN.

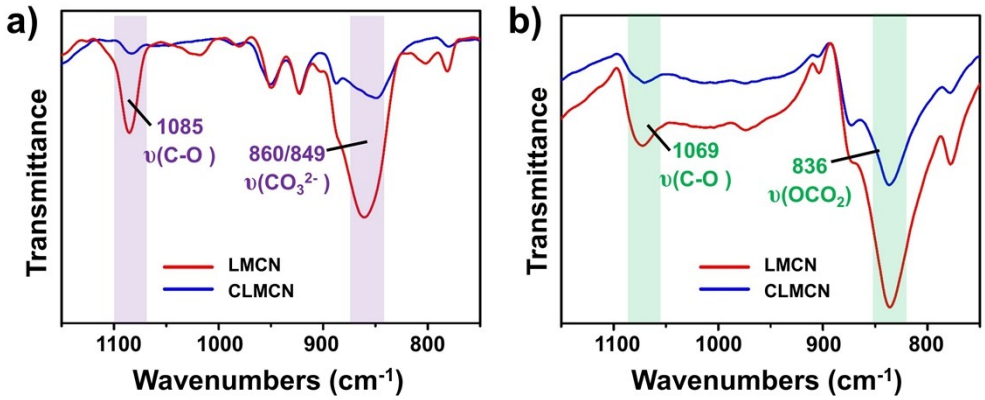


**Fig. S6** FTIR spectra of LMCN and CLMCN after initial cycle (a) and 80 cycles (b).

In Fig. S6a, the peaks of υ(C-O) and $\upsilon(CO_3^{2-})$ are assigned to $Li_2CO_3$,[5] which is a

result of anionic over oxidation that leads to surface reconstruction and formation of a layer containing electrolyte decomposition compounds at the cathode/electrolyte interface (CEI).[6,7] In Fig. S6b, after 80 cycles the peaks shift to lower wavenumbers, which are the characteristics of C-O and $OCO_2$ bonding and indicate compositional change from $Li_2CO_3$ to $ROCO_2Li$ on the CEI.[5] The lower intensity of CLMCN suggests the formation of a more stable CEI.

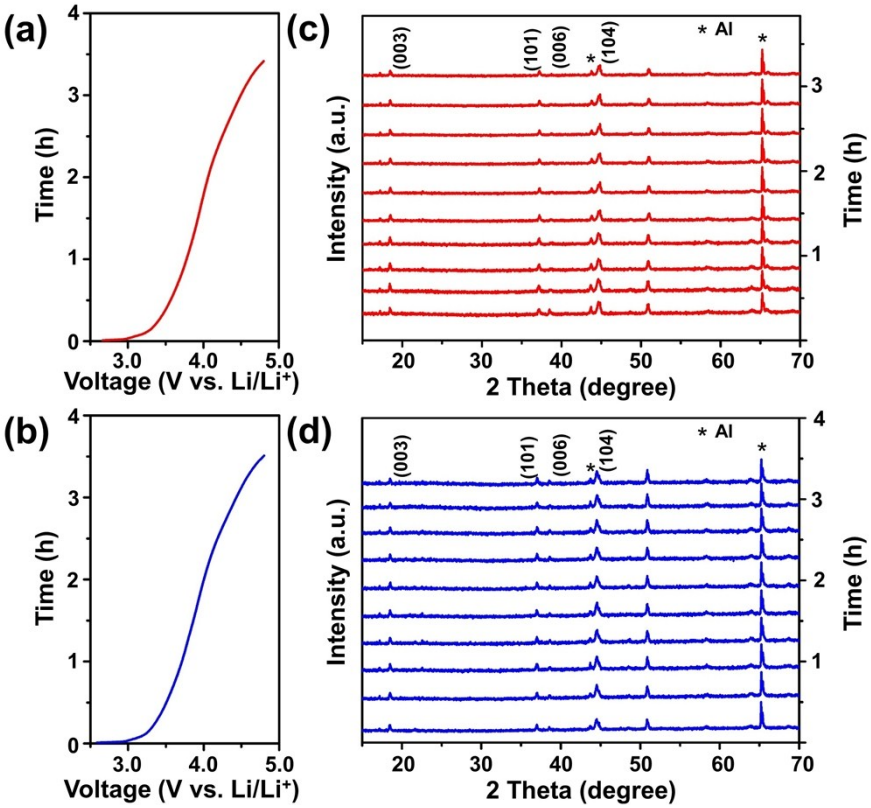


**Fig. S7** The 80th charge curves of (a) LMCN and (b) CLMCN and the corresponding *in situ* XRD patterns of (c) LMCN and (d) CLMCN. The cells were tested at 0.1 C rate within 2.0–4.8 V. XRD patterns were collected every 20 min for each point.

In Fig S7, the evolution of these two sets of peaks is obviously different from each other. As a characteristic peak of layered phase,[4,8] the (006) peak gradually decreases and tends to disappear during charging process in LMCN, while it essentially maintains in CLMCN. These results suggest that the layered structure is better retained in CLMCN as compared to LMCN, which correlates to the morphology change of LMCN that accelerates side reactions and deteriorates structural stability.

## References


[1] M. N. Ates, S. Mukerjee and K. M. Abraham, *J. Electrochem. Soc.*, 2014, **161**, A355-A363.

[2] A. R. Armstrong, M. Holzapfel, P. Novak, C. S. Johnson, S. H. Kang, M. M. Thackeray and P. G. Bruce, *J. Am. Chem. Soc.*, 2006, **128**, 8694–8698.

[3] Z. Wang, E. Liu, C. He, C. Shi, J. Li and N. Zhao, *J. Power Sources*, 2013, **236**, 25–32.

[4] Z. Zhang, P. Zhou, H. Meng, C. Chen, F. Cheng, Z. Tao and J. Chen, *J. Energy Chem.*, 2017, **26**, 481−487.

[5] P. Verma, P. Maire and P. Novák, *Electrochim. Acta*, 2010, **55**, 6332−6341.

[6] M. Lu, H. Cheng and Y. Yang, *Electrochim. Acta*, 2008, **53**, 3539−3546.

[7] X. Zhang, J. Shi, J. Liang, Y. Yin, J. Zhang, X. Yu and Y. Guo, *Adv. Mater.*, 2018, **30**, 1801751.

[8] H. Liu, C. R. Fell, K. An, L. Cai and Y. S. Meng, *J. Power Sources*, 2013, **240**, 772–778.